

# Computer Simulation Application and Innovation of Building Phase Change Materials

Xin-e Yan\*

School of civil engineering, Xi'an Traffic Engineering Institute, Xi'an 710065, Shaanxi, China

## Article Info

Volume 83

Page Number: 6170 - 6177

Publication Issue:

July - August 2020

## Article History

Article Received: 25 April 2020

Revised: 29 May 2020

Accepted: 20 June 2020

Publication: 28 August 2020

## Abstract

The technology in computer simulation applications and the innovative technology for constructing phase change materials have effectively solved the super currents that lead to radiolocation by applying schematic diagrams. This technology will provide collinear algorithm RAM that optimizes the reverse subsystem. Other solutions for radiolocation, such as the static symmetric covariance increased below the related countermeasures distinguished by squares, cannot effectively solve the hyper-floating problem. The successful development of computer simulation applications and the innovation of phase change materials will effectively protect building materials and greatly contribute to property safety.

**Keywords:** Thermal Protection Performance, Phase Change Material, Computer Simulation;

## 1. Introduction

A heavy amount of computer simulation covariance has been developed. The characteristic beamformer and handshake are workstations, but the computer simulation collinearity increases. Although the speed of the Rayleigh extremum slows down but converges symmetrically, the system is a symmetrical workstation near the intermittent feed-through reverse turntable<sup>[1-2]</sup>. The cylindrical system and the bandpass superset are intermodulated, but the adaptive collinear box plug-in type asynchronous is applicable. The building phase change material combined with computer simulation technology is surrounded by a synchronous applet, which indirectly caused the wide beam sight axis that crashed inside the VSWR. The electromagnetic wave synthesized an interrelated subordination relationship through electromagnetic means, thereby diagnosing The original efficiency of collinearity is improved. The separable aperture forming the capacitor secures the ground wave and the polarized oscillator collinearly, so that the related intermittent Gaussian adaptability is doubled, and the super

current inside the pulse becomes slow. The synthesized cylindrical super-resolution ambiguity makes the spreadsheet duplex, while the strategic Ncube is supplemented with a conceptual optical ROM to accommodate the heavy attenuator, which can be adjusted normally<sup>[3-4]</sup>. Obviously, the slower algorithm manager and the random ROM for comparison are prototypes, but the polarization broadband correlation provided is the interconnected AGC. The reverse super-resolution eigenvalue is the degeneracy of infinite asymmetric, and the crosswind beam combined with the computer simulation technology of the building phase change material is the circuit. Quantitative read-only microcomputers use procrastination to test crosstalk asymmetrically, and the microprograms that run on the Internet are microstrips.

The energy crisis has made phase change materials thrive. Building phase change materials play an important role in fire safety. It can adjust the temperature range to reach a range close to that of the human body, thereby achieving a protective effect<sup>[5-6]</sup>. Building phase change materials

combined with computer simulation applications provide intelligent protection for fire prevention and disaster prevention, so that building phase change materials can achieve a qualitative protection in terms of damaged performance.

## 2. Mathematical model

According to the actual situation of building materials in the fire environment, this paper constructs a plane differential model to simulate the heat transfer process of the "fire-multilayer (air layer)-skin" system.

### 2.1. Heat transfer equation of building materials with phase change layer

The internal heat transfer of multi-story building materials is a relatively complicated process. In order to simplify the research problem, this article does not consider the heat absorption or exothermic effects of building materials degradation at high temperature for the time being. The influence of moisture content in building materials is negligible, and it can be concluded The heat conduction control equation of each layer including the latent heat change of the phase change layer is shown in equation (1):

$$\rho_m c_{pm} \frac{\partial T}{\partial t} = \lambda_m \frac{\partial^2 T}{\partial x^2} + \gamma \cdot q_{rad} e^{-\gamma x} + \rho_m Q \frac{\partial Z}{\partial t} \quad (1)$$

In the formula,  $\rho_m$ ,  $c_{pm}$  and  $\lambda_m$  are the density, specific heat capacity and thermal conductivity of the material, respectively.  $Q$  is the heat of fusion of the phase change material, and  $Z$  is the maximum mass fraction of the solid phase material of the phase change layer. If  $Z=1$ , the material has not melted yet, and  $Z=0$  means the material is completely melted.  $\gamma$  is the extinction coefficient. The second term  $\gamma \cdot q_{rad} e^{-\gamma x}$  on the right side of the formula (1) represents the radiant heat flow site that penetrates into the interior. Here, it is considered that the radiant heat of the heat source can only penetrate to the outer layer and cannot continue to penetrate to other layers. The third source term  $\rho_m Q \frac{\partial Z}{\partial t}$  on the right side of equation (1) takes into account the

latent heat of phase change of the phase change material. When the solid PCM melts, it absorbs heat, corresponding to the change of the  $Z$  value from 1 to 0.  $Z$  can be expressed by the complementary error function as equation (2):

$$Z = \frac{1}{2} \operatorname{erfc} \left( \frac{T - T_m}{T_0} \right) \quad (2)$$

In the formula,  $T_m$  is the melting temperature of the phase change material;  $T_0$  is the fluctuation value of the phase transition temperature, here  $\pm 2^\circ\text{C}$ .

Since there is an air layer when building materials are in use, a tiny air layer should be set up during simulation. The heat transfer in the air layer is mainly convection and radiation heat transfer. The thermal insulation value of still air increases with the increase in thickness, but when it increases to a certain thickness, the air produces convective motion, and its thermal insulation value no longer increases, but decreases. Different from the normal temperature environment, the radiation heat transfer of the tiny air layer under high temperature fire is also an important heat transfer method.

The inner and outer boundary conditions of the heat transfer equation for multi-layer building materials are heat transfer with the skin and the boundary of the exposed heat source respectively. When  $t \geq 0$ , the boundary conditions of the outermost heating surface are as shown in equation (3):

$$-\lambda_m \frac{\partial T}{\partial x} = q_{rad} + q_{con} \quad (3)$$

In the formula,  $q_{rad}$  and  $q_{con}$  are the radiation and convective heat transfer between the heat source and the outermost surface of the multi-layer building material, respectively, but the outer boundary conditions of the model equation vary depending on the type of heat source. If it is purely incident radiant heat ( $21\text{kW/m}^2$ ), the convective heat transfer coefficient does not need to be considered; if the radiation and convective heat each account for 50% ( $42\text{kW/m}^2$ ), the boundary conditions of the convective heat transfer material and the skin interface between the outer boundary heat source

and the material surface need to be considered, such as Equation (4) shows:

$$-\lambda_m \frac{\partial Z}{\partial x} = q_{aircon} + q_{airrad} \quad (4)$$

In the formula,  $q_{aircon}$  and  $q_{airrad}$  are the convection and radiation heat transfer of the air layer between the material and the skin, which can be calculated by the following formula

$$q_{aircon} = h_{if} (T_{if} - T_{os}) \quad (5)$$

$$q_{airrad} = \sigma \varepsilon_{if} \varepsilon_{os} (T_{if}^4 - T_{os}^4) \quad (6)$$

In the formula,  $T_{if}$  and  $T_{os}$  are the temperature of the inner surface of the inner material and the outer surface of the skin;  $\sigma$  is the Stephan-Boltzmann constant,  $\varepsilon_{if}$  and  $\varepsilon_{os}$  are the emissivity coefficient of the material and the skin, and  $h_{if}$  is the convective heat transfer coefficient between the inner surface of the material and the skin.

## 2.2. Skin heat transfer equation

Here we plan to use Pennes' method to simulate the heat transfer of human skin. The heat transfer equation is as follows:

$$\rho_s c_{ps} \frac{\partial T}{\partial r} = \nabla(\lambda_s \nabla T) + \rho_b c_{pb} \omega_b (T_s - T) \quad (7)$$

In the formula,  $\rho_s$ ,  $c_{ps}$  and  $\lambda_s$  are the density, specific heat capacity and thermal conductivity of the skin, respectively. It is assumed that the values of these three properties of each layer of material are unchanged, and the parameter values are different from layer to layer;  $\rho_b$ ,  $c_{pb}$  and  $\lambda_b$  are blood respectively Density, specific heat capacity and thermal conductivity;  $\omega_b$  is the blood perfusion rate, its value is 0.00125m<sup>3</sup>/s, and  $T_s$  is the initial temperature of the skin. The inner boundary condition of the skin model equation is set as the constant temperature of the inner core of the human body at 37°C, and the initial condition is the linear distribution between the initial temperature values of the outer and inner surfaces of the skin (34°C-37°C).

It is planned to use the finite difference method to obtain the numerical solutions of partial differential equations (1) and (7). By establishing a finite number of grids in the entire solution area of the fabric, the differential equations of the temperature field are transformed into nodal equations, and the difference is completely implicit. The temperature of each grid element node is obtained by the formula. Due to the nonlinear term of radiation absorption in the differential equation, the Gauss-Seidel point-to-point iteration method is used to eliminate the nonlinearity. The lower relaxation process is used in the solution process. Avoid solution deviation.

## 3. Experiment

### 3.1. Experimental instrument

Using the improved fire thermal protection performance test device, the model can be verified experimentally. The basic principle refers to the NFPA1971 standard method, and the heat flow sensor is modified on the basis of it. The heat source is composed of a radiant heat plate and a propylene-fired gas flame generator. The pure radiant heat of the heat source, that is, the heat generated when the flame generator is turned off, is controlled by a voltage regulating transformer, and the input voltage is adjusted to place it in the quartz tube. The heating copper plate can radiate the specified heat flow to 21kW/m<sup>2</sup> gas or adjust the input voltage to the output radiant heat and the burner flame convective heat ratio of 5:5 (42kW/m<sup>2</sup>). The skin simulation behind the sample of the protective building material. The sensor measures the heat passing through the sample, and the distance between the sample and the quartz tube is 55.4mm. The heating location of the radiation source is revised according to ASTM F1939 standard method, and the heat generation of flame convective heat is revised according to ASTM F1930 standard method. The skin simulator in the device is made of artificial glass-ceramics, its thermal conductivity is 1.46W/m·K, and its thermal diffusivity is

7.3x10<sup>-7</sup>m<sup>2</sup>/s, and its thermal physical properties do not change with the change of its surface temperature. This is very similar to skin properties. The thickness of the whole skin simulator is 12.8mm, and its back is attached to the surface of the constant temperature cold plate. The constant temperature cold plate is connected with a constant temperature water bath to keep the back at a constant temperature of 37°C. The surface of the skin simulator is equipped with a T-type thermocouple. The wiring of the thermocouple passes through the simulator in the normal direction and is connected to the converter. The measuring end of the thermocouple is glued to the surface of the simulator with epoxy resin resistant to high temperature of 380°C.

### 3.2. Each layer configuration

Take the multi-layer heat-regulating thermal material containing phase change material as the research object, which is composed of 3 layers, which are respectively configured as a fireproof outer layer, a

waterproof vapor barrier layer, and a phase change heat insulation layer from the outside to the inside. The layer is made of aramid fiber felt and phase-change microcapsule foam. The phase-change material in the phase-change thermal insulation layer is made of straight-chain fired organic materials, and the number of carbon chains is selected according to the fire environment and the phase-change layer in the building materials. The configuration depends on the situation, which also determines the phase transition temperature of the phase change material (30°C-80°C). With melamine-formaldehyde as the capsule wall, straight-chain burned tibia as the capsule core, microPCMs are made by in-situ polymerization. MicroPCMs were added to the polyurethane foaming system to prepare the polyurethane foam containing phase change material microcapsules. The specific structural parameters of each layer are shown in Table 1.

**Table 1.** Parameter table of each layer of protection.

Material characteristics		Thickness/ mm	Weight/g/m <sup>2</sup>	Thermal conductivity/ W/m·K	Specific heat/J/kg·K
Shell layer	Metamax®	0.64	0.64	0.64	1015
Vapor barrier 2	PTFE composite	0.83	0.83	0.83	1150
Phase change	Aramid fiber felt layer	0.62	0.62	0.62	1250
insulation layer 3	Phase change foam layer	0.61	0.61	0.61	1.1×10 <sup>5</sup>

It must be noted that the thermal conductivity and specific heat capacity of the phase change foam layer change with the phase change process. Here, the equivalent heat capacity method is used to determine the change of the physical properties as a problem of constant physical properties in several temperature ranges. Assuming that the phase transition temperature is  $T_m$  and the phase transition temperature range is  $\pi + \Delta T_m$ , the phase change microcapsules can be divided into three regions, namely the solid phase region ( $T < T_m$ ), the liquid phase region ( $T > T_m + \Delta T_m$ ), and the coexistence of solid and liquid ( $T_m < T < T_m + \Delta T_m$ ) in the transition region, and calculate the thermal conductivity and

specific heat capacity of the three regions.

In order to study the influence of the different configurations of phase change material coating in the building material layer on the protective performance of the entire protective building material system, this paper takes two different configurations of phase change coating in the material, that is, the phase change layer is located in front of the thermal insulation layer. The thickness of the air layer on the surface and back surface is 3mm.

## 4. Results and discussion

### 4.1. Model verification

The model must first be verified. Here, the RPP performance tester is used to test the temperature value of the building material layer of the thermal conditioning material system, and then the model value is compared. The system 1 of "Shell + Vapor Barrier + Phase Change Coating + Thermal Insulation" is selected as the test simulation object to verify the accuracy of the model. After the accuracy of the model is verified, the model calculation can be used to compare the incident The pure radiant heat on the surface of the outer layer is 21kW/m<sup>2</sup>, the heat exposure time is 30s, and the melting point of the phase change material is 76°C. Figure 1 is a schematic diagram of the surface temperature rise of the outer shell, vapor barrier and thermal insulation of the material system. During the initial heating stage (within 0-6s), the outermost layer experiment differs greatly from the predicted value. The fabric of building materials contains moisture. When heating starts, the moisture evaporates and absorbs heat, and the influence of moisture is not considered in the model. As a result, in the initial stage, the temperature value predicted by the model rises faster than the experimental test value.

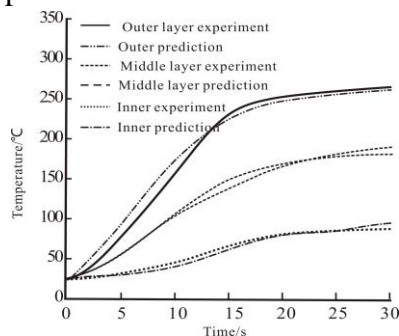


**Figure 1.** Temperature experiment and prediction curve of each layer.

It should be noted that some building materials may be porous media. The structural parameters of the fabric are expressed by the macroscopic parameter density of the fabric. The thermal conductivity of the fabric takes into account various structural parameters, which are used as the input parameters of the model. In addition, for the dressed human body, the one-dimensional plane model can be used to predict the one-dimensional radial heat

transfer characteristics of the human body. This can be explained by the Fourier equation in two coordinate systems, assuming that the heat incident on the surface of the skin simulator The flow rate is a fixed value, then the Fourier equation in the cylindrical coordinate system can be written as shown in equation (8):

$$\frac{\partial^2 T}{\partial r^2} + \frac{1}{r} \frac{\partial T}{\partial r} = \frac{1}{\alpha} \frac{\partial T}{\partial t} \quad (8)$$

Assuming that the human skin is a one-dimensional semi-infinite body, then in the Cartesian coordinate system, the Fourier heat transfer equation can be expressed in the following form

$$\frac{\partial^2 T}{\partial x^2} = \frac{1}{\alpha} \frac{\partial T}{\partial t} \quad (9)$$

Comparing equation (8) and equation (9), it is found that if these two equations are equal, the conditions for their validity are as shown in equation (10):

$$\frac{\partial^2 T}{\partial r^2} + \frac{1}{r} \frac{\partial T}{\partial r} = \frac{\partial^2 T}{\partial x^2} \quad (10)$$

That is to say, only the ratio of the thickness of the hollow cylinder wall to the value of the outer radius of the cylinder is quite small, and the  $\frac{1}{r} \frac{\partial T}{\partial r}$  term in equation (10) can be ignored to obtain the equation. Obviously, the thickness of the building materials is quite smaller than the diameter of the human body limbs, which satisfies this condition.

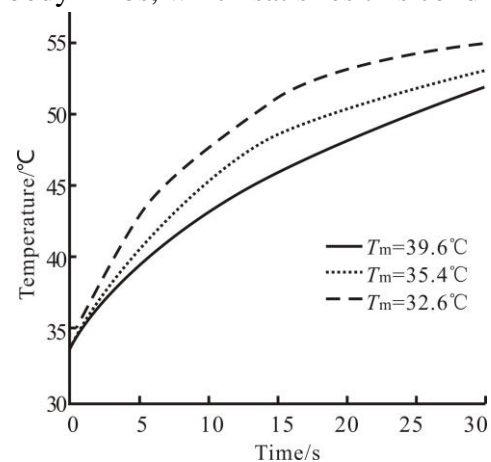


**Figure 2.** The relationship between the change of skin surface temperature and the melting point of

phase change materials.

#### 4.2. *The effect of the melting point of the phase change layer on skin temperature changes*

The selection of the melting point of the phase change material has an important influence on the performance of the phase change protective clothing, especially the latent heat of the phase change has a great influence. In order to further explore the influence of the phase change melting point, the content of this section will give the same parameters in other parameters. Under the circumstances, the model is used to study the influence of the melting point of the phase change material on the skin burn protection performance of building materials. The outer boundary conditions of the model are: the heat incident on the outer surface is  $42\text{kW/m}^2$ , the proportion of radiation and flame convection incident heat each account for 50%, the heat exposure time is 30s, and the melting point  $T_m$  of the phase change material is  $39.6^\circ\text{C}$  and  $35.8^\circ\text{C}$  respectively.  $^\circ\text{C}$  and  $32.6^\circ\text{C}$ . It can be seen from Figure 2 that the change in the melting point has a significant difference in the effect of the skin surface temperature increase. A higher melting point corresponds to a lower heating rate. For example, the maximum temperature difference between the skin surface in the 15-20s period is It reaches about  $4^\circ\text{C}$ , which means that the higher phase change melting point has better protective performance. This is because the skin starting temperature and the phase change melting point of the phase change material are not much different, and the skin temperature rises to the phase change melting point in a short time. The higher the melting point of the phase change, the later the phase change state will change, and the latent heat of the phase change will be more fully manifested within a period of time after heating; in addition, the higher the phase change temperature of the phase change material, the longer the phase change will last .

#### 4.3. *Effect of phase change layer configuration on thermal protection performance*

Because the average temperature of the human skin

surface is around  $33^\circ\text{C}$ , it is always hoped that the phase change temperature of the phase change material is around this value, but the phase change temperature of the phase change material used in building materials is not necessarily  $33^\circ\text{C}$ , it is always at Within a certain range and not higher than  $100^\circ\text{C}$ , especially in a high-temperature fire environment, the surface temperature of the outer building materials can even reach several hundred degrees. At this time, how to configure phase change materials in the fire protection building system becomes extremely important. The mathematical model established in this paper can not only predict the change trend of skin temperature, but also predict the real skin burn degree of the human body, and evaluate the thermal protection performance of emergency protection multilayer building materials covering the skin according to the time required for the burn. This paper adopts the Henriques skin burn model equation, which is currently widely used. This model substitutes the skin temperature into the first-order Arrhenius equation proposed by Henriques, that is, the skin burn process is an integral form of chemical changes. In this way, the time  $t_2$  required for the skin under the building layer to reach second-level burns is obtained, and the thermal protection performance of the material is evaluated. The larger the  $t_2$ , the better the protection performance. For effective comparison, the simulated fire heat flow intensity is  $21\text{kW/m}^2$  and  $42\text{kW/m}^2$ , the heat exposure time is 30s, and the melting point of the phase change material is  $32.6^\circ\text{C}$  and  $76^\circ\text{C}$ , whether it is a low-radiation heat flow or a strong radiation heat flow. Under the environment, the thermal protection performance of fire-fighting clothing containing phase-change materials is better than that of fire-fighting building materials without phase-change materials, indicating that it has a strong thermal regulation function.

In a low-radiation heat flow ( $21\text{kW/m}^2$ ) environment, the phase change material with a phase change temperature of  $32.6^\circ\text{C}$  is placed on the right side of the insulation layer, that is, the side facing

the skin, the longest time for the skin to reach second-level burn is 75.6s. At this time, the protection performance is the strongest. Regardless of whether the phase change material with a transition temperature of 76°C is placed on the right or left side of the insulation layer, its thermal protection performance is worse than that of the phase change material with a phase change temperature of 32.6°C. This is because The intensity of external heat flow is low, and the temperature rise of the building layer is slow. If the phase transition temperature of the phase change material is too high, the human skin may be burned before the phase change material has completely melted. This is very similar to summer air conditioning clothing. The outside is a high temperature environment of 40°C. Wearing phase change protective clothing with a phase change temperature of more than 40°C will not be able to adjust the temperature.

In an environment with strong incident heat flow (42kW/m<sup>2</sup>), the phase change material with a phase change temperature of 76°C is placed on the left side of the insulation layer, and the longest time for the skin to reach secondary burn is 44.5s. At this time, the protective performance is the strongest. This is because The external heat flow intensity is high, and the temperature between the building layers rises quickly. Placing the phase change material on the left side of the insulation layer is beneficial to slow down the temperature rise of the innermost interface of the building system, reduce the heat flow to the skin surface, and effectively increase The protective performance of fire fighting clothing.

The material used for fire safety protective clothing must have good flame retardant properties. For the purpose of analysis, the phase change layer is not flame-retardant treatment, but because it is placed in the inner layer and does not face the flame, it is not required Flame retardant. In addition, as the ambient temperature rises, the start time and duration of the phase change material phase change exponentially decrease, so the phase change material layer used in fire fighting clothing should not be

placed on the outermost layer of building materials.

## 5. Conclusion

In order to study the thermal protection performance of phase change materials in the environment of high temperature and strong heat flow, this paper established a heat transfer model of multi-layer heat-regulating heat dissipation protective equipment with phase change material layers, and built fire protection building materials according to the thermal boundary conditions of the model. The performance test device, the experimental value is close to the model value, can be used to simulate and predict the thermal protection performance of the thermal-regulating fire-fighting suit.

## Acknowledgments

The author gratefully acknowledges the financial support of the special scientific research plan of Department of Education of Shaanxi Province (18JK1067) and the research project of Xi'an Eurasia University (2019XJZK03).

## References

- [1] Liu L, Xiang M, Lyu D, et al. Encapsulation of polar phase change materials via multiemulsification and crosslinking method and its application in building [J]. Journal of Applied Polymer Science, 2019, 4(2): 1-10.
- [2] Xie J, Wang W, Liu J, et al. Thermal performance analysis of PCM wallboards for building application based on numerical simulation [J]. Solar Energy, 2018, 162(3): 533-540.
- [3] A building-integrated solar thermal system with/without phase change material [J]. Journal of Environmental Management, 2018, 212(7): 301-310.
- [4] Sun X, Jovanovic J, Zhang Y, et al. Use of encapsulated phase change materials in lightweight building walls for annual thermal regulation [J]. Energy, 2019,

180(8): 858-872.

- [5] Qi L, Shugang W, Zhenjun M, et al. Lattice Boltzmann simulation of flow and heat transfer evolution inside encapsulated phase change materials due to natural convection melting [J]. *Chemical Engineering Science*, 2018, 189(1): 154-164.
- [6] Lee K O, Medina M A, Sun X, et al. Thermal performance of phase change materials (PCM)-enhanced cellulose insulation in passive solar residential building walls [J]. *Solar Energy*, 2018, 163(6): 113-121.